Downlink Specific Linear Equalization for Frequency Selective CDMA Cellular Systems [1]

Thomas P. Krauss, William J. Hillery, and Michael D. Zoltowski
1285 School of Electrical and Computer Engineering
Purdue University
West Lafayette, IN 47907-1285
e-mail: krauss@purdue.edu, hilleryw@ecn.purdue.edu, mikedz@ecn.purdue.edu
Phone: 765-494-3512
FAX: 765-494-0880

Invited Paper for Special Issue of Journal of VLSI Signal Processing, May 2001

Abstract

We derive and compare several linear equalizers for the CDMA downlink under frequency selective multipath conditions: minimum mean-square error (MMSE), zero-forcing (ZF), and RAKE. MMSE and ZF equalizers are designed based on perfect knowledge of the channel. The downlink specific structure involves first inverting the multipath channel to restore the synchronous multi-user signal transmitted from the base-station at the chip-rate, and then correlating with the product of the desired user's channel code times the base-station specific scrambling code once per symbol to decode the symbols. ZF equalization restores orthogonality of the Walsh-Hadamard channel codes on downlink; MMSE does so approximately but also avoids excessive noise gain. We compare MMSE and ZF to the traditional matched filter (also known as the RAKE receiver). Our formulation generalizes for the multi-channel case as might be derived from multiple antennas and/or over-sampling with respect to the chip-rate. The optimal symbol-level MMSE equalizer is derived and slightly out-performs the chip-level but at greater computational cost. An MMSE soft hand-off receiver is derived and simulated. Average BER for a class of multi-path channels is presented under varying operating conditions of single-cell and edge-of-cell, coded and un-coded BPSK data symbols, and uncoded 16-QAM. These simulations indicate large performance gains compared to the RAKE receiver, especially when the cell is fully loaded with users. Bit error rate (BER) performance for the chip-level equalizers is well predicted by approximate SINR expressions and a Gaussian interference assumption.

[1] This research was supported by the Air Force Office of Scientific Research under grant no. F49620-00-1-0127 and the Texas Instruments DSP University Research Program.

1 Introduction

We further investigate the properties and performance of linear equalizers for receivers designed specifically for the CDMA downlink. The system in consideration uses orthogonal Walsh-Hadamard channel codes and a base-station dependent scrambling code or "long code," similar to the CDMA standard IS-95 and proposed standard cdma2000. The channel is frequency-selective multipath fading with delay-spread equal to a significant fraction of the symbol period. We examine BPSK and 16-QAM symbols with QPSK spreading; however the results here-in also apply to systems with symbols and spreading drawn from other constellations.

Mobile receivers in current CDMA cellular systems employ a matched filter (also known as a RAKE receiver) which combines the energy from multiple paths across time, and space (if spatial or polarization diversity is employed). The matched filter is ideal when there are no interfering users [1]. In the CDMA forward link, there are many other users being transmitted through the same channel although with different spreading codes. The current CDMA standards (IS-95) and standards proposals (cdma2000 and UMTS W-CDMA) for third generation (3G) systems all employ orthogonal Walsh-Hadamard channel codes on the downlink. This means that in a flat faded situation, upon despreading with a correctly synchronized spreading code of the desired user, all interference from other same-cell users is completely eliminated. Major problems arise when the fading is not flat, which is true often in urban wireless systems at the high chip rates specified in 3G systems. Major problems also arise when the user is near the edge of a cell and receiving significant out-of-cell interference, regardless of whether the fading is flat or not.

In this paper we derive the MMSE chip estimator for the two base-station case. The results can be easily extended to more base-stations; in practice at most three base-stations will be received. We simulate equalizers for a class of frequency-selective fading channels, both near one base-station so the out-of-cell inteference is negligible, and mid-way between two base-stations where the mobile experiences significant out-of-cell interference. For the edge-of-cell case, we derive and analyze a "soft-hand-off" mode in which the desired user's data is transmitted simultaneously from two base-stations, as well as the "typical" mode where the second base-station is considered interference. We assess the cases of one and two receive antennas and compare them. Our results indicate that MMSE significantly out-performs RAKE, and that two antennas significantly out-perform a single receive antenna with oversampling. These results hold both for soft hand-off and normal operation although, as expected, soft hand-off enhances performance.

One fundamental question this work tries to address is whether adding a second antenna at the mobile is worth the associated costs and difficulties. In future cellular systems, the physical link from base-station to handset or other mobile data terminal will be a major bottleneck. Employing spatial diversity through multiple antennas, *at the mobile-station*, can possibly eliminate this bottleneck. There is great hesitation to include multiple antennas at the mobile-station because of the extreme pressures to keep handsets cheap and low power. However the cost of bandwidth is also competing head-on and at some point may be more expensive than multiple antenna hardware. Our simulations show the potential a multiple antenna equalizer has for reducing interference and hence increasing system performance, range and capacity. Broadband wireless access will require exponential increases in system performance, so it is only a matter of time before the idea of two or more antennas at the mobile-station is embraced and put into practice.

Some relevant papers on linear chip equalizers that restore orthogonality of the Walsh-Hadamard channel codes and hence suppress multi-user access interference (MAI) are [2, 3, 4, 5, 6, 7, 8, 9, 10, 11, 12]. Of these, [2, 3, 5, 6] consider a single antenna with oversampling, while the others address the multi-channel case (antenna arrays). The interference from other base-stations is addressed only in Ghauri and Slock [4], Frank and Visotsky [3], and later by us in [10, 12]. Of those listed, "soft-hand-off" mode has been considered only in [10, 12]. References [6] and [7] simulate the use of OVSF channel codes in which some users are assigned multiple Walsh-Hadamard channel codes to transmit data at lower spreading factors. In [9] and [13] we argue that zero-forcing (ZF) equalization in this CDMA down-link context, even in the multi-antenna case, suffers from poor channel conditioning for sparse channels; this result is confirmed in the present work. In [12] we present results for convolutionally encoded BPSK, and uncoded 16-QAM constellations.

In this paper, as in References [3],[4], and [5], the channel and noise power are assumed known (i.e., channel estimation error is neglected), as well as time synchronization with the long scrambling code. However, as suggested in [8] where the channel is blindly estimated via the "cross-relation" of Xu, Liu, Tong, and Kailath [14], channel estimation is extremely important and its failure leads to disastrous results for equalization. Using the exact channel in simulation and analysis leads to an informative upper bound on the performance of these methods, but must be understood as such. Reference [5] takes a very similar approach to ours but with a different channel model: 2- or 4-path Rayleigh with much smaller delay spread as would be found in indoor environments. Also their equalizers are single antenna with 4 times oversampling. Frank and Visotsky [3] consider adaptive equalization based on the pilot channel, which solves the problem of not knowing the channel as well as handling time variation. [15] proposes a subspace method for blind channel identification specifically for the CDMA downlink with long scrambling codes; however they assume the symbol interval is longer than the delay spread, which may not always be true for 3G CDMA systems. The assumption we make that the channel is unchanging might be the case only over a short time interval. For adaptive versions of linear chip equalizers for CDMA downlink, see [3] and [6] and references in [5]. Note for the equalizers studied herein, as well as for blind channel identification and adaptive equalization based on the pilot symbols as proposed elsewhere, synchronization with the long code is required.

As in [10] and [12], we derive performance measures conditioned on the channel in the form of receiver SINR; from this a BER estimate is obtained based on a Gaussian approximation. This approximation is shown to be a highly accurate prediction of the uncoded BER. [3] and [4] also present performance analysis in the form of SINR expressions for the multiple base-station case.

Linear multiuser detection for CDMA systems is treated fairly thoroughly in Verdu's text [1] and compared to the optimal multi-user detector. The optimal detector is non-linear with complexity that increases exponentially with the number of users and delay spread. Our work may be considered an investigation into several sub-optimal multi-user detectors for the specific case of receiving sets of synchronous users through different frequency selective fading channels (from the different base-stations), with orthogonal spreading and a base-station-dependent long code. These linear equalizers are much less computationally complex than the optimal detector, but have performance which significantly improves on the standard matched-filter (RAKE). Reference [16] presents several ZF and MMSE detectors for the frequency selective channel, although not specifically for the downlink.

2 Data and Channel Models

The impulse response for the $i-th$ antenna channel, between the k^{th} base-station transmitter and the mobile-station receiver, is

$$h_i^{(k)}(t) = \sum_{\ell=0}^{N_a-1} h_i^{(k)}[\ell] p_{rc}(t-\tau_\ell) \quad i=1,2, k=1,2 \tag{1}$$

$p_{rc}(t)$ is the composite chip waveform (including both the transmit and receive low-pass filters) which we assume has a raised-cosine spectrum. N_a is the total number of delayed paths or "multipath arrivals," some of which may have zero or negligible power without loss of generality.

The channel we consider for this work consists of $N_a = 17$ equally spaced paths $0.625\mu s$ apart ($\tau_0 = 0$, $\tau_1 = 0.625\mu s$, $\ldots$); this yields a delay spread of at most $10\mu s$, which is an upper bound for most channels encountered in urban cellular systems. The spacing of $0.625\mu s$ is motivated by the software channel simulator SMRCIM [17] which utilizes this spacing for urban cellular environments. We use this spacing in our simulations; however the methods presented in this work do not require any specific spacing of the τ_ℓ or that they are evenly spaced. The simulations employ a class of channels with 4 equal-power random coefficients with arrival times picked randomly from the set $\{\tau_0, \tau_1, \ldots, \tau_{16}\}$; the rest of the coefficients $h_i^{(1)}[\ell]$ are zero. Once the 4 arrival times have been picked at random and then sorted, the first and last arrival times are forced to be at 0 and the maximum delay spread of $10\mu s$ respectively. The coefficients are equal-power, complex-normal random variables, independent of each other. The arrival times at antennas 1 and 2 associated with a given base-station are the same, but the coefficients are independent. See Figure 1 for a plot of a typical channel's impulse response, sampled at the chip rate.

The "multi-user chip symbols" for base-station k, $s^{(k)}[n]$, may be described as

$$s^{(k)}[n] = c_{bs}^{(k)}[n] \sum_{j=1}^{N_u^{(k)}} \sum_{m=0}^{N_s-1} \alpha_j^{(k)} b_j^{(k)}[m] c_j^{(k)}[n - N_c m] \tag{2}$$

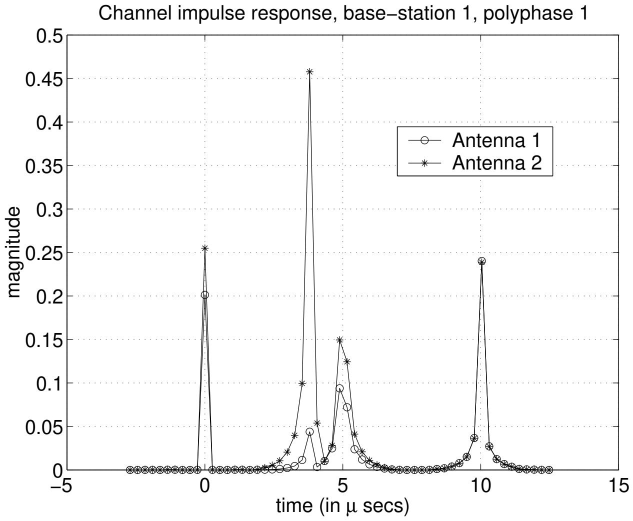

Figure 1: Typical impulse response for base-station 1, sampled at the chip rate. Includes tails from chip waveform.

where the various quantities are defined as follows: k is the base-station index; $c_{bs}^{(k)}[n]$ is the base-station dependent long code; $\alpha_j^{(k)}$ is the j^{th} user's gain; $b_j^{(k)}[m]$ is the j^{th} user's bit/symbol sequence; $c_j^{(k)}[n]$, $n = 0, 1, ..., N_c - 1$, is the j^{th} user's channel (short) code; N_c is the length of each channel code (assumed the same for each user); $N_u^{(k)}$ is the total number of active users; N_s is the number of bit/symbols transmitted during a given time window. The signal received at the i^{th} antenna (after convolving with a matched filter impulse response having a square-root raised cosine spectrum) from base-station k is

$$y_i^{(k)}(t) = \sum_n s^{(k)}[n] h_i^{(k)}(t - nT_c) \quad i = 1, 2 \tag{3}$$

where $h_i^{(k)}(t)$ is as defined in Eqn. (1). The total received signal at the mobile-station is simply the sum of the contributions from the different base-stations plus noise:

$$y_i(t) = y_i^{(1)}(t) + y_i^{(2)}(t) + \eta_i(t) \quad i = 1, 2. \tag{4}$$

$\eta_i(t)$ is a noise process assumed white and Gaussian prior to coloration by the receiver chip-pulse matched filter. Without loss of generality, only two base-stations are assumed; the subsequent sections may be extended in a straight forward manner to more than two.

For the first antenna, we oversample the signal $y_1(t)$ in Eqn. (4) at twice the chip-rate to obtain $y_1[n] = y_1(nT_c)$ and $y_2[n] = y_1(\frac{T_c}{2} + nT_c)$. These discrete-time signals have corresponding impulse responses $h_1^{(k)}[n] = h_1^{(k)}(t)|_{t=nT_c}$ and $h_2^{(k)}[n] = h_1^{(k)}(t)|_{t=\frac{T_c}{2}+nT_c}$ for base-stations $k = 1, 2$.

For the second antenna, we also oversample the signal $y_2(t)$ in Eqn. (4) at twice the chip-rate to obtain $y_3[n] = y_2(nT_c)$ and $y_4[n] = y_2(\frac{T_c}{2} + nT_c)$. These discrete-time signals have corresponding impulse responses $h_3^{(k)}[n] = h_2^{(k)}(t)|_{t=nT_c}$ and $h_4^{(k)}[n] = h_2^{(k)}(t)|_{t=\frac{T_c}{2}+nT_c}$ for base-stations $k = 1, 2$.

Let M denote the total number of chip-spaced channels due to both receiver antenna diversity and/or oversampling. When two times oversampling is employed, $M = 2$ channels if only one antenna is used, while $M = 4$ channels if both antennas are used. For some simulations, two antennas are employed with no oversampling (in which case $M = 2$).

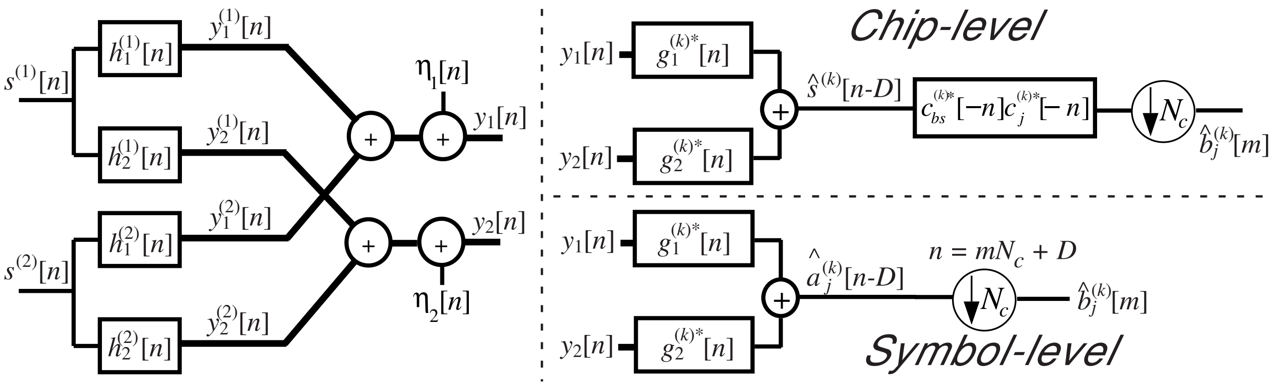

Figure 2: MMSE "Multi-User Chip Symbol" Estimator for k^{th} Base-Station, two channel case (either one antenna with oversampling, or two antennas with no oversampling).

3 Estimate of Multi-User Synchronous Sum Signal

In addition to the matched-filter, we also consider two other types of estimators for the synchronous sum signal at the chip rate $s[n]$: zero-forcing (ZF), and minimum mean-square error (MMSE). These "chip-level" equalizers are shown in Figure 2 (single antenna case). They estimate the multi-user synchronous sum signal for either base-station 1 or 2, and then correlate with the desired user's channel code times that base-station's long code.

To derive the chip-level equalizers (both ZF and MMSE), it is useful to define signal vectors and channel matrices based on the equalizer length N_g. The "recovered" chip signal will be $\hat{s}^{(k)}[n-D] = \mathbf{g}^{(k)H}\mathbf{y}[n]$ for some delay D, where $\mathbf{g}^{(k)}$ is the $MN_g \times 1$ chip-level equalizer for base-station k, $k = 1, 2$. The $MN_g \times 1$ vectorized received signal is given by

$$\mathbf{y}[n] = \mathbf{H}^{(1)}\mathbf{s}^{(1)}[n] + \mathbf{H}^{(2)}\mathbf{s}^{(2)}[n] + \boldsymbol{\eta}[n] \tag{5}$$

where

$$\mathbf{s}^{(k)}[n] = \left[s^{(k)}[n], s^{(k)}[n-1], \ldots, s^{(k)}[n-(N_g+L-2)]\right]^T \tag{6}$$

$$\mathbf{H}^{(k)} = \begin{bmatrix} \mathbf{H}_1^{(k)} \\ \vdots \\ \mathbf{H}_M^{(k)} \end{bmatrix} \tag{7}$$

$\mathbf{H}_i^{(k)}$ is the $N_g \times (L + N_g - 1)$ convolution matrix

$$\mathbf{H}_i^{(k)} = \begin{bmatrix} h_i^{(k)}[0] & 0 & \dots & 0 \\ h_i^{(k)}[1] & h_i^{(k)}[0] & 0 & 0 \\ \vdots & \ddots & \ddots & \ddots \\ h_i^{(k)}[L-1] & h_i^{(k)}[L-2] & \ddots & h_i^{(k)}[0] \\ 0 & h_i^{(k)}[L-1] & \ddots & h_i^{(k)}[1] \\ \vdots & \ddots & \ddots & \ddots \\ 0 & 0 & 0 & h_i^{(k)}[L-1] \end{bmatrix}^T . \tag{8}$$

Equation (5) is more compactly written as

$$\mathbf{y}[n] = \boldsymbol{\mathcal{H}}\mathbf{s}[n] + \boldsymbol{\eta}[n] \tag{9}$$

where

$$\boldsymbol{\mathcal{H}} = \left[\mathbf{H}^{(1)} \ \vdots \ \mathbf{H}^{(2)}\right] \tag{10}$$

and

$$\mathbf{s}[n] = \left[\mathbf{s}^{(1)T}[n] \quad \mathbf{s}^{(2)T}[n]\right]^T . \tag{11}$$

Note that in some of our simulations, only one base-station is considered, and the second base-station is assumed to have negligible power. This case is included in our notation by simply letting the coefficients of base-station 2's channel go to zero.

3.1 BLUE (ZF) Estimate of Multi-User Synchronous Sum Signal

For multiple channels obtained either through over-sampling and/or multiple antennas, there are infinitely many zero-forcing equalizers provided the channel matrix $\boldsymbol{\mathcal{H}}$ is left-invertible. Besides the requirement that the $MN_g \times 2(N_g + L - 1)$ matrix $\boldsymbol{\mathcal{H}}$ is tall, left invertibility requires that the subchannels of each channel have no common zeros. Assuming well conditioned channels, the optimal choice among the infinitely-many ZF equalizers is to minimize the noise gain, which is obtained with the "best linear unbiased estimate" (BLUE) equalizer; this equalizer is also presented in [6].

Specifically, to design a ZF equalizer we solve a constrained optimization problem:

$$\begin{gathered} \underset{\mathbf{g}^{(k)}}{\text{Minimize}} \quad E\{|\mathbf{g}^{(k)H}\boldsymbol{\eta}[n]|^2\} \\ \text{subject to } \mathbf{g}^{(k)H}\boldsymbol{\mathcal{H}}\mathbf{s}[n] = s^{(k)}[n-D], \forall\, n \end{gathered} \tag{12}$$

In matrix form this becomes

$$\begin{gathered} \underset{\mathbf{g}^{(k)}}{\text{Minimize}} \quad \mathbf{g}^{(k)H}\mathbf{R}_{\eta\eta}\mathbf{g}^{(k)} \\ \text{subject to } \mathbf{g}^{(k)H}\boldsymbol{\mathcal{H}} = \boldsymbol{\delta}_D^{(k)T} \end{gathered} \tag{13}$$

where $\mathbf{R}_{\eta\eta} = E\{\boldsymbol{\eta}[n]\boldsymbol{\eta}[n]^H\}$ is the noise covariance matrix, $\boldsymbol{\delta}_D$ of size $(N_g + L - 1) \times 1$ is all zeroes except for unity in the $(D+1)^{th}$ position (so that $\boldsymbol{\delta}_D^T\mathbf{s}^{(k)}[n] = s^{(k)}[n-D]$) and

$$\boldsymbol{\delta}_D^{(k)T} = \begin{cases} \left[\boldsymbol{\delta}_D^T \quad \mathbf{0}^T_{(N_g+L-1)\times 1}\right], & k = 1 \\ \left[\mathbf{0}^T_{(N_g+L-1)\times 1} \quad \boldsymbol{\delta}_D^T\right], & k = 2 \end{cases}$$

The objective and constraint can be combined into a single unconstrained objective function by introducing a Lagrange vector $\boldsymbol{\lambda}$:

$$\mathbf{f}(\mathbf{g}^{(k)}, \boldsymbol{\lambda}) = \mathbf{g}^{(k)H}\mathbf{R}_{\eta\eta}\mathbf{g}^{(k)} + (\mathbf{g}^{(k)H}\boldsymbol{\mathcal{H}} - \boldsymbol{\delta}_D^{(k)T})\boldsymbol{\lambda} \tag{14}$$

$\mathbf{f}(\mathbf{g}^{(k)}, \boldsymbol{\lambda})$ is a real function with complex vector arguments; to minimize it, it is useful to employ Brandwood's complex gradient $\nabla_{\mathbf{g}^*}$ [18]:

$$\nabla_{\mathbf{g}^*}\mathbf{f}(\mathbf{g}^{(k)}, \boldsymbol{\lambda}) = \mathbf{R}_{\eta\eta}\mathbf{g}^{(k)} + \boldsymbol{\mathcal{H}}\boldsymbol{\lambda} = \mathbf{0} \tag{15}$$

$$\mathbf{g}^{(k)} = -\mathbf{R}_{\eta\eta}^{-1}\boldsymbol{\mathcal{H}}\boldsymbol{\lambda} \tag{16}$$

The gradient with respect to $\boldsymbol{\lambda}$ simply yields the constraint that $\mathbf{g}^{(k)H}\boldsymbol{\mathcal{H}} - \boldsymbol{\delta}_D^{(k)T} = 0$. Then plugging the necessary form for $\mathbf{g}^{(k)}$ into the constraint we have

$$-\boldsymbol{\lambda}^H\boldsymbol{\mathcal{H}}^H\mathbf{R}_{\eta\eta}^{-1}\boldsymbol{\mathcal{H}} = \boldsymbol{\delta}_D^{(k)T} \tag{17}$$

from which we solve for the Lagrange vector

$$\boldsymbol{\lambda} = -(\boldsymbol{\mathcal{H}}^H\mathbf{R}_{\eta\eta}^{-1}\boldsymbol{\mathcal{H}})^{-1}\boldsymbol{\delta}_D^{(k)} \tag{18}$$

The final BLUE solution is thus given by

$$\mathbf{g}^{(k)} = \mathbf{R}_{\eta\eta}^{-1}\boldsymbol{\mathcal{H}}(\boldsymbol{\mathcal{H}}^H\mathbf{R}_{\eta\eta}^{-1}\boldsymbol{\mathcal{H}})^{-1}\boldsymbol{\delta}_D^{(k)} \tag{19}$$

For the channels we simulated we sometimes encountered singular or near-singular channel matrices, and frequently when a single antenna is employed with 2 times oversampling as opposed to 2 antennas. To avoid conditioning problems, a small diagonal loading of 10^{-9} was applied prior to matrix inversion in the simulations.

The ZF equalizer depends on the particular delay D chosen for the right-hand side $\boldsymbol{\delta}_D$ and also the equalizer length N_g. For a fixed equalizer length, the "best choice" equalizer is the one that has smallest noise gain $\mathbf{g}^{(k)H}\mathbf{R}_{\eta\eta}\mathbf{g}^{(k)}$. It is not necessary to compute all $L + N_g - 1$ possible equalizers corresponding to each of the possible delays. Instead, we note that $\mathbf{g}^{(k)H}\mathbf{R}_{\eta\eta}\mathbf{g}^{(k)} = \boldsymbol{\delta}_D^{(k)T}(\boldsymbol{\mathcal{H}}^H\mathbf{R}_{\eta\eta}^{-1}\boldsymbol{\mathcal{H}})^{-1}\boldsymbol{\delta}_D^{(k)}$ which is the $(D+1)^{th}$ diagonal element of $(\boldsymbol{\mathcal{H}}^H\mathbf{R}_{\eta\eta}^{-1}\boldsymbol{\mathcal{H}})^{-1}$ (or the $(D+1) + (N_g + L - 1)$ element if $k = 2$). Hence our method of computing the equalizer $\mathbf{g}^{(k)}$ with the best delay is:

- compute the matrix inverse $(\boldsymbol{\mathcal{H}}^H\mathbf{R}_{\eta\eta}^{-1}\boldsymbol{\mathcal{H}})^{-1}$,
- find the smallest element of the diagonal of the appropriate block (either the upper-left block for $k = 1$ or the lower-right block for $k = 2$),
- multiply the column corresponding to that element by the matrix $\mathbf{R}_{\eta\eta}^{-1}\boldsymbol{\mathcal{H}}$.

Our simulation experience has found that optimizing over D led to a 1-2 dB improvement in average BER performance over simply choosing the reasonable "centered" delay of $D = \lfloor (N_g + L - 1)/2 \rfloor$.

3.2 MMSE Estimate of Multi-User Synchronous Sum Signal

The MMSE estimate of the synchronous sum signal in Equation 2 is $\hat{s}^{(k)}[n-D] = \mathbf{g}^{(k)H}\mathbf{y}[n]$ where $\mathbf{g}^{(k)}$ minimizes the MMSE criterion:

$$\min_{\mathbf{g}^{(k)}} E\{|\mathbf{g}^{(k)H}(\boldsymbol{\mathcal{H}}\mathbf{s}[n] + \boldsymbol{\eta}[n]) - \boldsymbol{\delta}_D^T \mathbf{s}^{(k)}[n]|^2\} \tag{20}$$

where $\boldsymbol{\delta}_D$ is all zeroes except for unity in the $(D+1)-th$ position (so that $\boldsymbol{\delta}_D^T \mathbf{s}^{(k)}[n] = s^{(k)}[n-D]$). In contrast to MMSE *symbol* estimates, we here estimate the *chip-rate signal* $s^{(k)}[n]$ as transmitted from the desired base-station, and follow this with correlation and summation with the long code times channel code to obtain the symbol. This procedure works by approximately restoring the orthogonality of the Walsh-Hadamard codes, but allowing a residual amount of interference from other users to achieve reduction in noise gain relative to an exact ZF solution.

We assume unit energy signals, $E\{|s^{(k)}[n]|^2\} = 1$, and furthermore that the chip-level symbols $s^{(k)}[n]$ are independent and identically distributed, $E\{\mathbf{s}[n]\mathbf{s}^H[n]\} = \mathbf{I}$. This is the case if the base-station dependent long codes, $c_{bs}^{(k)}[n]$, are treated as iid sequences, a very good assumption in practice. The equalizer $\mathbf{g}^{(k)}$ which attains the minimum is

$$\mathbf{g}^{(k)} = \left(\boldsymbol{\mathcal{H}}\boldsymbol{\mathcal{H}}^H + \mathbf{R}_{\eta\eta}\right)^{-1} \mathbf{H}^{(k)}\boldsymbol{\delta}_D. \tag{21}$$

Note this is the standard solution to the Wiener-Hopf equations $\mathbf{R}_{yy}\mathbf{g}^{(k)} = \mathbf{r}_{sy}$ where

$$\mathbf{R}_{yy} = E\mathbf{y}[n]\mathbf{y}^H[n] = \boldsymbol{\mathcal{H}}\boldsymbol{\mathcal{H}}^H + \mathbf{R}_{\eta\eta} \tag{22}$$

and

$$\mathbf{r}_{sy} = Es^*[n-D]\mathbf{y}[n] = \mathbf{H}^{(k)}\boldsymbol{\delta}_D. \tag{23}$$

The MMSE is

$$\mathrm{MMSE} = 1 - \boldsymbol{\delta}_D^T \mathbf{H}^{(k)H} \left(\boldsymbol{\mathcal{H}}\boldsymbol{\mathcal{H}}^H + \mathbf{R}_{\eta\eta}\right)^{-1} \mathbf{H}^{(k)}\boldsymbol{\delta}_D. \tag{24}$$

The MMSE equalizer is also a function of the delay D. The MMSE may be computed for each $D, 0 \le D \le N_g + L - 2$ with only one matrix inversion (which has to be done to form $\mathbf{g}^{(k)}$ anyway). Once the D yielding the smallest MMSE is determined, the corresponding equalizer $\mathbf{g}^{(k)}$ may be computed without further matrix inversion or system solving. Our simulation experience has found that optimizing over D led to a slight improvement in average BER performance over simply fixing D at $\lfloor (N_g + L - 1)/2 \rfloor$. The improvement was less than that experienced by the BLUE equalizer, implying the BLUE equalizer is more sensitive to choice of delay.

3.3 Asymptotic Behaviour of MMSE

In the matrix inversion lemma for matrices of the form

$$(A + BCD)^{-1} = A^{-1} - A^{-1}B(DA^{-1}B + C^{-1})^{-1}DA^{-1} \tag{25}$$

(see e.g. [19]), let $A = \mathbf{R}_{\eta\eta}, B = \boldsymbol{\mathcal{H}}, C = \mathbf{I}, D = \boldsymbol{\mathcal{H}}^H$. From this we obtain

$$\left(\boldsymbol{\mathcal{H}}\boldsymbol{\mathcal{H}}^H + \mathbf{R}_{\eta\eta}\right)^{-1}\boldsymbol{\mathcal{H}} = \mathbf{R}_{\eta\eta}^{-1}\boldsymbol{\mathcal{H}}\left(\boldsymbol{\mathcal{H}}^H\mathbf{R}_{\eta\eta}^{-1}\boldsymbol{\mathcal{H}} + \mathbf{I}\right)^{-1}. \tag{26}$$

Recognizing that $\mathbf{H}^{(k)}\boldsymbol{\delta}_D = \boldsymbol{\mathcal{H}}\boldsymbol{\delta}_D^{(k)}$, the MMSE equalizer of Equation (21) is equivalent to

$$\mathbf{g}^{(k)} = \mathbf{R}_{\eta\eta}^{-1}\boldsymbol{\mathcal{H}}\left(\boldsymbol{\mathcal{H}}^H\mathbf{R}_{\eta\eta}^{-1}\boldsymbol{\mathcal{H}} + \mathbf{I}\right)^{-1}\boldsymbol{\delta}_D^{(k)}. \tag{27}$$

This last expression shows that the MMSE equalizer gives us the best of both worlds: at low SNR, the MMSE equalizer

$$\mathbf{g}_{MMSE} \propto \mathbf{R}_{\eta\eta}^{-1}\boldsymbol{\mathcal{H}}\boldsymbol{\delta}_D^{(k)} \tag{28}$$

acts like a "pre-whitened" RAKE receiver, and therefore benefits from the diversity gains of the multipath-incorporating matched filter. At high SNR,

$$\mathbf{g}_{MMSE} \propto \mathbf{R}_{\eta\eta}^{-1}\boldsymbol{\mathcal{H}}\left(\boldsymbol{\mathcal{H}}^H\mathbf{R}_{\eta\eta}^{-1}\boldsymbol{\mathcal{H}}\right)^{-1}\boldsymbol{\delta}_D^{(k)} \tag{29}$$

acts like the BLUE (ZF) Equalizer of Equation (19) and hence can completely eliminate the MAI because the orthogonality of the channel codes is restored. Note however that for channels that have close to common zeroes, the performance of the ZF equalizer does not approach the performance of the MMSE at high SNR. Because of the instability incurred in inverting the ill-conditioned matrix $\boldsymbol{\mathcal{H}}\mathbf{R}_{\eta\eta}^{-1}\boldsymbol{\mathcal{H}}^H$, the ZF equalizer performs much worse than the MMSE (as seen in the simulations).

3.4 Performance Analysis

To obtain the symbol estimate for the chip-spaced equalizers, we assemble the chip signal estimate into a length N_c vector and form its inner product with the length N_c channel code times the appropriate portion of the base-station long code:

$$\hat{b}_j^{(k)}[m] = \mathbf{c}_j^{(k)H}[m]\hat{\mathbf{s}}^{(k)}[n] \tag{30}$$

Here and for the remainder of this section, the chip index n is a specific function of the symbol index m and delay D: $n = (m+1)N_c + D - 1$. $\mathbf{c}_j^{(k)}[m]$ is the length N_c channel code vector of the k^{th} base-station's j^{th} user times the long code of that base-station,

$$\mathbf{c}_j^{(k)}[m] = \begin{bmatrix} c_{bs}^{(k)}[N_c m + N_c - 1]c_j^{(k)}[N_c - 1] \\ c_{bs}^{(k)}[N_c m + N_c - 2]c_j^{(k)}[N_c - 2] \\ \vdots \\ c_{bs}^{(k)}[N_c m + 1]c_j^{(k)}[1] \\ c_{bs}^{(k)}[N_c m]c_j^{(k)}[0] \end{bmatrix} \tag{31}$$

The composite channel formed by the convolution of channel and equalizer, and summed together, is a time-invariant, SISO (single-input single-output) FIR system of length $L + N_g - 1$. Let this impulse response, for the channel between the ℓ^{th} base-station and the equalizer "tuned" to the k^{th} base-station's channel, be denoted $h_{eq}^{(\ell,k)}[n]$

$$h_{eq}^{(\ell,k)}[n] = \sum_{i=1}^{M} \sum_{l=0}^{L-1} h_i^{(\ell)}[l] g_i^{(k)*}[n-l], n = 0, \ldots, L + N_g - 2$$

Here, the equalizer coefficients $g_i^{(k)}[n]$ comprise the equalizer vector

$$\mathbf{g}^{(k)} = [\mathbf{g}_1^{(k)T} \ \cdots \ \mathbf{g}_M^{(k)T}]^T \tag{32}$$

where

$$\mathbf{g}_i^{(k)} = [g_i^{(k)}[0], g_i^{(k)}[1], \ldots, g_i^{(k)}[N_g - 1]]^T \quad i = 1, \ldots, M. \tag{33}$$

All of the composite responses may be decomposed into a delay D term, plus a residual impulse response, or "ISI" contribution:

$$h_{eq}^{(\ell,k)}[n] = h_{eq}^{(\ell,k)}[D]\delta[n-D] + \tilde{h}_{eq}^{(\ell,k)}[n].$$

For the zero-forcing criterion, the ISI portion $\tilde{h}_{eq}^{(\ell,k)}[n]$ will be zero.

Assume for the moment that we seek to estimate the symbol from user 1, transmitted from base-station $k = 1$. The symbol estimate in Equation (30) becomes

$$\begin{aligned} \hat{b}_1^{(1)}[m] &= \mathbf{c}_1^{(1)H}[m]\hat{\mathbf{s}}^{(1)}[n] \\ &= \left\{2N_c h_{eq}^{(1,1)}[D]\alpha_1^{(1)}\right\} b_1^{(1)}[m] + \\ &\mathbf{c}_1^{(1)H}[m] \left(\tilde{\boldsymbol{\mathcal{H}}}_{eq}^{(1,1)}\mathbf{s}^{(1)}[n] + \boldsymbol{\mathcal{H}}_{eq}^{(2,1)}\mathbf{s}^{(2)}[n] + \boldsymbol{\eta}_{eq}^{(1)}[n]\right) \end{aligned} \tag{34}$$

where $\boldsymbol{\mathcal{H}}_{eq}^{(\ell,k)}$ is the $N_c \times (N_c + L + N_g - 2)$ convolution matrix for composite impulse response $h_{eq}^{(\ell,k)}[n]$, and

$$\boldsymbol{\mathcal{H}}_{eq}^{(\ell,k)} = \boldsymbol{\mathcal{H}}_{eq,D}^{(\ell,k)} + \tilde{\boldsymbol{\mathcal{H}}}_{eq}^{(\ell,k)} \tag{35}$$

$\boldsymbol{\mathcal{H}}_{eq,D}^{(\ell,k)}$ has only one non-zero diagonal, which by construction picks out exactly that portion of $\mathbf{s}_1^{(k)}[n]$ corresponding to the m^{th} symbol. $\boldsymbol{\eta}_{eq}^{(1)}[n]$ is the post-equalization noise vector.

Here we have used the fact that $c_j^{(k)}[n] = \pm 1$ and $c_{bs}^{(k)}[n] = \pm 1 \pm \sqrt{-1}$ (the QPSK long code gives rise to the factor of 2 in Equation (34)). Also, due to orthogonality of the Walsh-Hadamard channel codes, $\mathbf{c}_1^{(1)H}[m]\boldsymbol{\mathcal{H}}_{eq,D}^{(1,1)}\mathbf{s}_{2:N_u}^{(1)}[n] = 0$, that is, all same-cell users on the direct path are cancelled. Rewrite (34) as "signal" term plus an "interference plus noise" term denoted as γ:

$$\hat{b}_1^{(1)}[m] = (2N_c h_{eq}^{(1,1)}[D]\alpha_1^{(1)})b_1^{(1)}[m] + \gamma. \tag{36}$$

The SINR is given by

$$\begin{aligned} \text{SINR} &= E\{|2N_c h_{eq}^{(1,1)}[D]\alpha_1^{(1)} b_1^{(1)}[m]|^2\}/E\{|\gamma|^2\} \\ &= 4(N_c\alpha_1^{(1)})^2|h_{eq}^{(1,1)}[D]|^2/E\{|\gamma|^2\} \end{aligned} \tag{37}$$

where we have used the fact that $E\{|b_j^{(k)}[m]|^2\} = 1$. The expectation in the denominator can be shown to contain a weighted sum of products of the long code evaluated at four different indices (e.g., $E\{c_{bs}[n_1]c_{bs}^*[n_2]c_{bs}[n_3]c_{bs}^*[n_4]$ and reduces to

$$E\{|\gamma|^2\} = 2N_c(2||\tilde{h}_{eq}^{(1,1)}[n]||^2 + 2||h_{eq}^{(2,1)}[n]||^2 + \mathbf{g}^{(1)H}\mathbf{R}_{\eta\eta}\mathbf{g}^{(1)}). \tag{38}$$

Note in practice with BPSK symbols that the constant times symbol $(2N_c h_{eq}^{(1,1)}[D]\alpha_1^{(1)})b_1^{(1)}[m]$ is real while the noise and interference term γ is complex. The power of the real part of the interference plus noise $E\{|\text{real}(\gamma)|^2\}$ is simply half of the power of the complex term:

$$E\{|\text{real}(\gamma)|^2\} = E\{|\gamma|^2\}/2. \tag{39}$$

Hence,

$$\text{SINR}_{\text{BPSK}} = 2\ \text{SINR} = \frac{4(N_c\alpha_1^{(1)})^2|h_{eq}^{(1,1)}[D]|^2}{N_c(2||\tilde{h}_{eq}^{(1,1)}[n]||^2 + 2||h_{eq}^{(2,1)}[n]||^2 + \mathbf{g}^{(1)H}\mathbf{R}_{\eta\eta}\mathbf{g}^{(1)})}. \tag{40}$$

The hard decision of the symbol is taken to be 1 if $real(\hat{b}_1^{(1)}[m])$ is positive and -1 otherwise. Assuming the real part of the interference is Gaussian by a central-limit argument with a large number of interferers, the bit error rate (BER) for BPSK information symbols is

$$\text{BER} = Q(\sqrt{\text{SINR}_{\text{BPSK}}}) \tag{41}$$

where $Q(x) = \frac{1}{\sqrt{2\pi}}\int_x^\infty e^{-\alpha^2/2}d\alpha$. This approximation has been empirically determined to be valid even for as few as 8 users where the Gaussian assumption might be tenuous (see Figure 11 in the Simulations section). Note that this BER is valid as an approximation for both MMSE and RAKE and any other linear equalizer, and is exact for ZF equalizers.

4 Soft Hand-Off Mode

For soft hand-off mode, the desired user's symbols are modulated onto one of the channel codes at each base-station. At the receiver, two equalizers are designed, one for each base-station: we attempt to estimate $s^{(1)}[n]$ the multi-user synchronous sum signal from base-station one, AND $s^{(2)}[n]$ the multi-user synchronous sum signal from base-station two, via individual equalizers. The output of each of the two chip-level equalizers is correlated with the desired user's channel code times the corresponding base-station's long code (see Figure 2), yielding two symbol estimates. These two signal estimates are optimally combined for the soft-hand-off mode. For the MMSE equalizer, the total delay of the signal, D, through both channel and equalizer, was chosen to minimize the MSE of the equalizer; this was done for both equalizers.

For deriving the combining coefficients, we have two bit estimates of the form:

$$\begin{aligned} \hat{b}_1^{(1)}[m] &= a_1 b_1[m] + \gamma_1 \\ \hat{b}_1^{(2)}[m] &= a_2 b_1[m] + \gamma_2 \end{aligned} \tag{42}$$

We seek combining coefficients w_1, w_2 in order to minimize

$$E\{|w_1 \hat{b}_1^{(1)}[m] + w_2 \hat{b}_1^{(2)}[m] - b_1[n]|^2\} \tag{43}$$

Assuming a_1, a_2 are known real constants and γ_1, γ_2 are zero-mean independent random variables with known power ($E\{|\gamma_i|^2\} = \sigma_{\gamma_i}^2$), the weights are given by

$$\begin{bmatrix} w_1 \\ w_2 \end{bmatrix} = \frac{1}{(a_1^2 + \sigma_{\gamma_1}^2)(a_2^2 + \sigma_{\gamma_2}^2) - (a_1 a_2)^2} \begin{bmatrix} a_1 \sigma_{\gamma_2}^2 \\ a_2 \sigma_{\gamma_1}^2 \end{bmatrix} \tag{44}$$

While technically γ_1, γ_2 are not independent, with many users and iid scrambling codes, their correlation will be very small and may be ignored in practice.

Note that this soft hand-off analysis could also be applied to the symbol-level equalizer of Section 6, as well as the chip-level equalizers (MMSE, RAKE, and ZF).

5 RAKE Receiver

The above performance analysis and soft hand-off receiver apply also to the RAKE receiver, which is simply a multipath-incorporating matched filter. In particular, the RAKE can be viewed as a chip-spaced filter matched to the channel, followed by correlation with the long code times channel code (see Figure 2). Note, in practice, these operations are normally reversed, but reversal is allowed due to short-time LTI assumptions. Specifically, to apply the above results to the RAKE receiver, let $N_g = L$ and $g_i^{(k)}[n] = h_i^{(k)}[L-n], n = 0, \ldots, L-1, i = 1, \ldots, M$.

6 Symbol-level Equalizer

In this section we present what we call the "symbol-level" MMSE estimator. This estimator depends on the user index and symbol index, and hence varies from symbol to symbol. The FIR estimator that we derive here is a simplified version of that presented in [20] where in our case, all the channels and delays from a given base-station are the same. The equalizer is much more computationally complex and complicated when all the different users travel through different channels with different delays. The conclusions reached in that paper apply equally well here, namely that FIR MMSE equalization always performs at least as well as the "coherent combiner" (that is, the RAKE receiver). This type of symbol-level receiver has also been presented in [16], although again not specifically for the CDMA downlink.

The symbol-level equalizer differs from the chip-level equalizer in that the base-station and Walsh-Hadamard codes do not appear explicitly in the block diagram (see Figure 2). Instead, the codes become incorporated into the equalizer itself. To derive the equalizer, we first define $a_j^{(k)}[n]$ as the bit sequence $b_j^{(k)}[m]$ upsampled by N_c: $a_j^{(k)}[n] = b_j^{(k)}[m]$ when $n = mN_c$ and $a_j^{(k)}[n] = 0$ otherwise. We wish to estimate $b_j^{(k)}[m]$ directly and we do this by finding

$$\min_{\mathbf{g}^{(k)}} E\{|\hat{a}_j^{(k)}[n-D] - a_j^{(k)}[n-D]|^2\} \tag{45}$$

where the minimization is done only when $n-D=mN_c$. As in the chip-level case, $\hat{a}_j^{(k)}[n-D]=\mathbf{g}^{(k)H}\mathbf{y}[n]$ where $\mathbf{y}[n]$ is given by Eq. (9). Setting $n=mN_c+D$, the MSE is minimized yielding

$$\mathbf{g}^{(k)}[m]=(\boldsymbol{\mathcal{H}}\mathbf{R}_{SS}[mN_c+D]\boldsymbol{\mathcal{H}}^H+\mathbf{R}_{\eta\eta})^{-1}\boldsymbol{\mathcal{H}}\mathbf{R}_{bS}[m] \tag{46}$$

where

$$\begin{aligned}\mathbf{R}_{SS}[n] &= E\{\mathbf{s}[n]\mathbf{s}^H[n]\} && (47)\\ \mathbf{R}_{bS}[m] &= E\{b_j^*[m]\mathbf{s}[mN_c+D]\}. && (48)\end{aligned}$$

Once again, this is the standard solution to the Wiener-Hopf equations $\mathbf{R}_{yy}[m]\mathbf{g}^{(k)}[m]=\mathbf{r}_{by}[m]$ where

$$\mathbf{R}_{yy}[m]=E\mathbf{y}[mN_c+D]\mathbf{y}^H[mN_c+D]=\boldsymbol{\mathcal{H}}\mathbf{R}_{SS}[mN_c+D]\boldsymbol{\mathcal{H}}^H+\mathbf{R}_{\eta\eta} \tag{49}$$

and

$$\mathbf{r}_{by}[m]=Eb_j^*[m]\mathbf{y}[mN_c+D]=\boldsymbol{\mathcal{H}}\mathbf{R}_{bS}[m]. \tag{50}$$

We now proceed to derive expressions for $\mathbf{R}_{SS}[n]$ and $\mathbf{R}_{bS}[m]$. Using Eq. (11),

$$\mathbf{R}_{SS}[n]=\begin{bmatrix}\mathbf{R}_{SS}^{(11)}[n] & \mathbf{R}_{SS}^{(12)}[n]\\ \mathbf{R}_{SS}^{(21)}[n] & \mathbf{R}_{SS}^{(22)}[n]\end{bmatrix} \tag{51}$$

where $\mathbf{R}_{SS}^{(pq)}[n]=E\{\mathbf{s}^{(p)}[n]\mathbf{s}^{(q)H}[n]\}$. We assume here that the desired user is only transmitted by base station k. We also assume that the base-station and Walsh-Hadamard codes are deterministic and known so that the only random elements in $\mathbf{s}[n]$ are the transmitted bits. The reason for this change of assumptions from the chip-level case is that if we assume the long code is i.i.d. for the symbol-level equalizer, the right-hand-side $\mathbf{r}_{by}[m]$ vanishes because of the independence of the symbol and long code and the zero-mean property of the long code. Then $E\{s^{(k)}[n]s^{(j)*}[m]\}=0$ for $k\neq j$ and any n and m, so $\mathbf{R}_{SS}^{(12)}[n]=\mathbf{R}_{SS}^{(21)}[n]=\mathbf{0}$. The $(i,j)^{th}$ element of $\mathbf{R}_{SS}^{(kk)}[n]$ is $S_{ij}^{(kk)}[n]=E\{s^{(k)}[n+1-i]s^{(k)*}[n+1-j]\}$. When $i=j$, $S_{ij}^{(kk)}[n]=1$. When $i\neq j$,

$$S_{ij}^{(kk)}[n]=\begin{cases}\frac{1}{2N_u^{(k)}}B_{ij}[n]W_{ij}^{(k)}[n], \text{ when}\\ \qquad (n+1-i)\mathrm{mod}N_c=(n+1-j)\mathrm{mod}N_c\\ 0 \qquad \text{otherwise}\end{cases} \tag{52}$$

where

$$B_{ij}[n]=c_{bs}^{(k)}[n+1-i]c_{bs}^{(k)*}[n+1-j], \tag{53}$$

$$W_{ij}^{(k)}[n]=\sum_{p=1}^{N_u^{(k)}}c_p^{(k)}[(n+1-i)\mathrm{mod}N_c]c_p^{(k)}[(n+1-j)\mathrm{mod}N_c] \tag{54}$$

with

$$B_{ij}[n]\in\{\pm 2,\pm 2\sqrt{-1}\}\ \forall\, i,j. \tag{55}$$

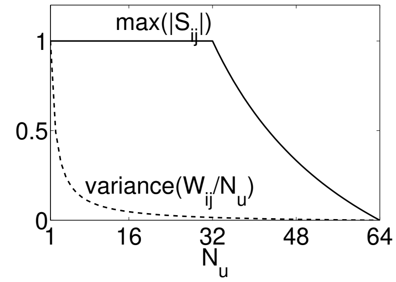

Figure 3: Bound on the potentially non-zero off-diagonal elements of $R_{SS}[n]$ $[N_c = 64]$.

With fixed m and n, $m \neq n$, note that $\left[c_1^{(k)}[m], \ldots, c_{N_c}^{(k)}[m]\right]^T$ and $\left[c_1^{(k)}[n], \ldots, c_{N_c}^{(k)}[n]\right]^T$ are two *different* rows of the Hadamard matrix. The element-by-element (Schur) product of these two rows is also a row of the Hadamard matrix containing $(N_c/2)$ 1's and $(N_c/2)$ -1's. So

$$|W_{ij}^{(k)}[n]| \leq \begin{cases} N_u & N_u = 1, \ldots, N_c/2 \\ N_c - N_u & N_u = N_c/2+1, \ldots, N_c \end{cases} \tag{56}$$

Therefore, when $i \neq j$ and $(n+1-i)\mathrm{mod}N_c = (n+1-j)\mathrm{mod}N_c$,

$$|S_{ij}^{(kk)}[n]| \leq \begin{cases} 1 & N_u^{(k)} = 1, \ldots, N_c/2 \\ N_c/N_u^{(k)} - 1 & N_u^{(k)} = N_c/2+1, \ldots, N_c \end{cases} \tag{57}$$

This bound is plotted as a function of $N_u^{(k)}$ in Fig. 3. Note that when $N_u^{(k)} = N_c$, $S_{ij}^{(kk)}[n] = 0$ for all $i \neq j$, so $\mathbf{R}_{SS}^{(kk)}[n] = \mathbf{I}$. If we assume that the $N_u^{(k)}$ Walsh codes are chosen randomly when $N_u^{(k)} < N_c$, it can be shown that $W_{ij}^{(k)}[n]/N_u^{(k)}$ is a linear function of a hypergeometric random variable. Its variance is $N_u^{(k)}(N_c - N_u^{(k)})/(N_c - 1)$. Therefore, those off-diagonal elements which are not zero have zero mean and a very small variance as shown in the plot in Fig. 3. For nearly all values of $N_u^{(k)}$, the variance is clearly quite small. So in all cases, we may well approximate $\mathbf{R}_{SS}^{(kk)}[n]$ by $\mathbf{I}$ in Eq. (46) yielding

$$\mathbf{g}^{(k)}[m] = (\boldsymbol{\mathcal{H}}\boldsymbol{\mathcal{H}}^H + \mathbf{R}_{\eta\eta})^{-1}\boldsymbol{\mathcal{H}}\mathbf{R}_{bS}[m] \tag{58}$$

We will see through simulation that this approximation works quite well when compared to the "exact" equalizer constructed with a time-varying $\mathbf{R}_{SS}$.

The i^{th} element of $\mathbf{R}_{bS}[m]$ is (with $n = mN_c + D$):

$$E\{b_j^{(k)*}[m]s[n+1-i]\} = \begin{cases} c_{bs}^{(k)}[n+1-i]c_j^{(k)}[D+1-i], \text{ for} \\ \qquad 0 \leq D+1-i \leq N_c - 1 \\ 0 \qquad \text{otherwise} \end{cases} \tag{59}$$

With D satisfying $N_c - 1 \leq D \leq L + N_g - 2$, the entire Walsh code for the desired user appears in $\mathbf{R}_{bS}[m]$ and

$$\mathbf{R}_{bS}[m] = \begin{bmatrix} \mathbf{0}_{D+1-N_c} & \mathbf{c}_j^{(k)}[m] & \mathbf{0}_{L+N_g-2-D} \end{bmatrix}^T \tag{60}$$

where $\mathbf{c}_j^{(k)}[m]$ is defined in Equation (31).

While the equalizer varies from symbol to symbol due to variation in both $\mathbf{R}_{SS}[n]$ and $\mathbf{R}_{bS}[m]$, by approximating $\mathbf{R}_{SS}[n]$ by $\mathbf{I}$, the variation is confined to $\mathbf{R}_{bS}[m]$.

7 Simulations

A wideband CDMA forward link was simulated similar to one of the options in the US cdma2000 proposal [21]. The spreading factor is $N_c = 64$ chips per bit. The chip rate is 3.6864 MHz ($T_c = 0.27\mu s$), 3 times that of IS-95. The data symbols for each user are BPSK unless otherwise stated, and are spread with a length 64 Walsh-Hadamard function. The signals for all the users are of equal power and summed synchronously. The sum signal is scrambled with a multiplicative QPSK spreading sequence ("scrambling code") of length 32768 similar to the IS-95 standard; the offset into this code is determined by the base-station and is the same for all users of a given base-station.

The signals were sampled at a factor of eight times the chip rate in order to perform accurate matched-filtering with the square-root chip pulse filter. The channel $h_i^{(k)}(t)$ was the exact continuous time convolution of a square-root raised cosine (beta = .22) pulse $p_{sr}(t)$ with the discrete impulse response $h_i^{(k)}[\ell]$. This was then sampled at eight times the chip rate. The noise was white at the different antennas, also generated at eight times the chip rate. The sum of the contributions from the two base-stations, and the noise, was filtered with a chip matched filter, also at eight times the chip rate; this gave the proper noise coloration, manifested as correlation between different polyphase channels from the same antenna. The different polyphase channels were formed by sub-sampling the eight times oversampled received signal at the chip rate; the 0th polyphase started at samples 0,8,16, etc, while the 1st polyphase started at 4,12,20, etc. The square-root raised cosine pulse used for both the generation of $h_i^{(k)}(t)$ and at the receiver was truncated at 5 chip intervals to the right and left of the origin.

The BER results are averaged over 500 different channels and among the different users for varying SNRs. Theoretical BER results based on Equation 41 in Section 3.4 are shown. The channels were generated according to the model presented in Section 2. For the two base-station case, the channels are scaled so that the total energy from each of the two base-stations is equal at the receiver. Specifically,

$$\sum_{m=1}^{M} E\{|y_m^{(1)}[n]|^2\} = \sum_{m=1}^{M} E\{|y_m^{(2)}[n]|^2\}. \tag{61}$$

In the one base-station case, the channel from the second base-station is set to zero. "SNR" is defined to be the ratio of the sum of the average powers of the received signals from both base-stations, to the average noise power, after chip-matched filtering. Note this definition of SNR is more amenable to the soft hand-off mode since the second base-station is considered "signal energy" instead of "interference energy." "SNR per user per symbol" is SNR multiplied by the spreading factor and divided by the number of users, which for 64 users is the same as the SNR.

For ZF and MMSE, the total delay of the signal, D, through both channel and equalizer, was chosen to minimize the MSE of the equalizer.

7.1 One Base-station

We first present results for a single base-station, in which the mobile unit is near the base and out-of-cell interference is negligible. Figure 4 shows the average BER performance for a two antenna system with no oversampling. All 64 users are active and equal power. The MMSE and ZF equalizers are compared with the RAKE receiver. Equalizers of length $N_g = 57$ (equal to the channel length including tails of the chip waveform), and twice that length $N_g = 114$ were simulated.

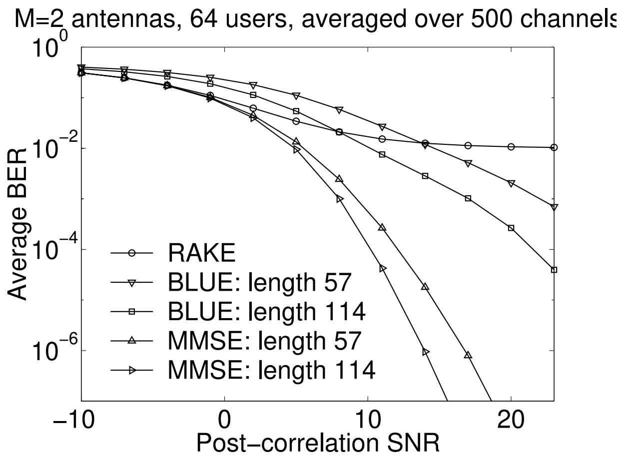

Figure 4: Comparison of RAKE, BLUE (ZF), and MMSE

From the curves of Figure 4 we see that the RAKE receiver benefits from diversity gains at lower SNR, while the ZF equalizer benefits from the orthogonality of codes at moderate to high SNR. We observe that the RAKE receiver's average performance saturates at high SNR, so that BERs below .01 are not possible no matter how little noise is present; this is due to the interference that the matched filter allows to pass in this frequency selective channel. The average performance for the MMSE is much better than RAKE or ZF. Both MMSE and ZF benefit from longer equalizers.

As expected, the MMSE equalizer approaches the RAKE at low SNR. However, the MMSE does not approach the ZF at high SNR. This may be partially explained by the next figure, Figure 5. This figure shows that the ZF equalizer has a large degree of variability in performance in the class of channels simulated. The worst channels for the ZF equalizer have performance so bad that the mean BER is dominated by these bad channels at high SNR. These few bad channels correspond to a channel matrix $\mathcal{H}$ that is very ill conditioned corresponding to near common zeros, and hence it cannot be said that the MMSE equalizer is approximately ZF equalizer in this case at high SNR. For a large class of channels, the ZF equalizer exhibits a BER that falls off more like the MMSE; the *median* BER (the 50^{th} percentile) of the ZF and MMSE equalizers is off by at most 3 dB, whereas the *mean* BER is 10 dB or more worse for ZF than MMSE at high SNR. In contrast, the MMSE exhibits less variability in performance across the different channels (Figure 6). Given the poor average performance of the ZF equalizer we will not consider its use for the remainder of the simulations.

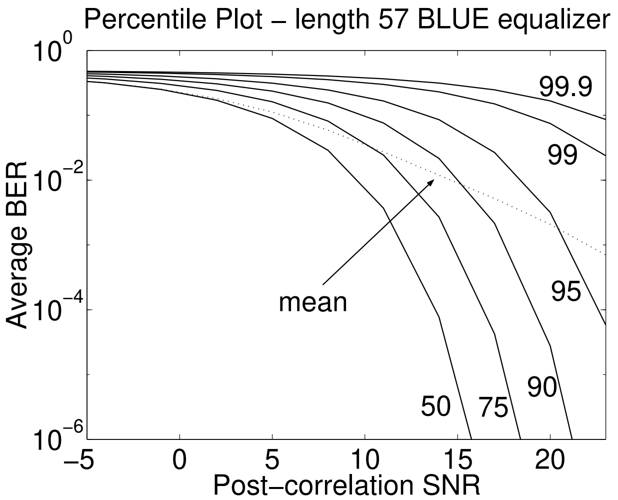

Figure 5: Percentile Plot of ZF Equalizer BER.

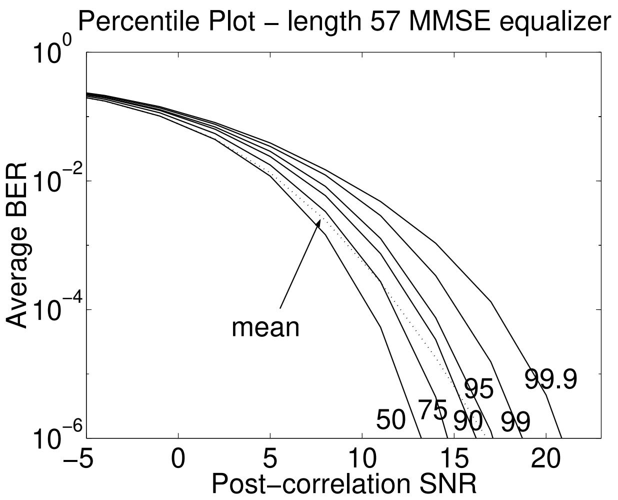

Figure 6: Percentile Plot of MMSE Equalizer BER.

Note that RAKE suffers less from MAI with fewer users (and hence has a lower BER floor), while ZF is the same no matter how many users are active. This is clearly seen in the plots for 16 and 32 users in [9] which are not included here. The MMSE slightly degrades as the number of users in the cell is increased, however it still allows a substantial improvement over the conventional RAKE receiver. This is shown for MMSE versus RAKE in the 8 users plot of Figure 13. This validates the use of our i.i.d. sequence assumption for the scrambling code along with the MMSE criterion for estimating the synchronous sum signal.

7.2 Two Base-stations

For both the RAKE and MMSE, two chip-level equalizers are designed, one for each base-station restoring the multi-user synchronous sum signal from that base-station. The output of each of the two chip-level equalizers is correlated with the desired user's channel code times the corresponding base-station's long code (see Figure 2), obtaining two symbol estimates. These two signal estimates are weighted and summed for the soft-hand-off mode as developed in Section 4.

Simulations were performed for both "saturated cells," that is, all 64 possible channel codes active in each cell, as well as lightly loaded cells with 8 channel codes active in each cell. The MMSE equalizer length was set to $N_g = 100$. Two antennas were employed with two times oversampling per antenna for a total of $M = 4$ chip-spaced channels.

The results of the simulations are plotted in Figure 7 for 8 users per cell, and in Figure 8 for 64 users per cell. Note in both cases, the RAKE receiver's performance flattens out at high SNR due to the MAI. This effect is more severe when many users are present; in fact, a minimum BER of only .01 to .1 is possible with the RAKE receiver when $N_u = 64$ channel codes are active, regardless of how high the SNR.

The MMSE significantly out performs the RAKE receiver. To illustrate this more clearly, Figures 9 and 10 plot the difference in SNR between the RAKE and MMSE receivers as a function of target uncoded BER. For both normal and soft hand-off modes of operation, the RAKE requires much more power than the MMSE receiver. This is more pronounced when there are more users, and when soft hand-off is unavailable. MMSE equalization allows operation in SNR regions that would be impossible with RAKE receivers - especially the case when a large number of channel codes are active relative to the spreading factor.

Figure 11 compares the theoretical BER approximation using the Gaussian assumption of Equation 41 and the derived SINR expression. This figure illustrates that, even for only 8 users where the Gaussian assumption might not hold very well, the theory and simulation results are very well matched. The simulation results ran 100 bits through each channel at each SNR point and for each user (for a total of 6400 bits per channel times 500 channels = 3.2 million bits for 64 users, or 0.4 million for 8 users). This plot also shows that the MMSE equalizer degrades much less dramatically than RAKE when the number of active channel codes increases.

7.3 Symbol-level Versus Chip-Level

To analyze the performance of the symbol-level equalizer as presented in Section 6, we simulated a receiver near the base-station so that out-of-cell interference is negligible. Two receive antennas are employed with no oversampling. Two equalizer lengths were simulated: for chip-level, $N_g = 57$ and 114, while for symbol-level, the length is chosen $N_c - 1$ longer. Since the chip-level equalizer is followed by correlation with the channel code times long code, its effective length is $N_g + N_c - 1$; hence, a fair comparison between

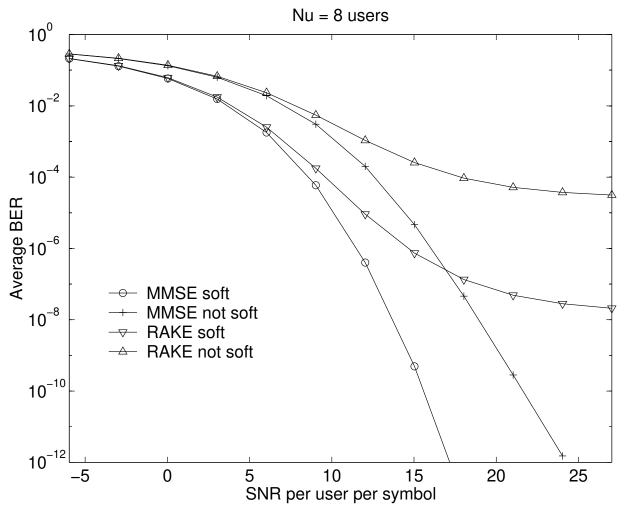

Figure 7: Uncoded BER results, 8 users, 2 base-stations

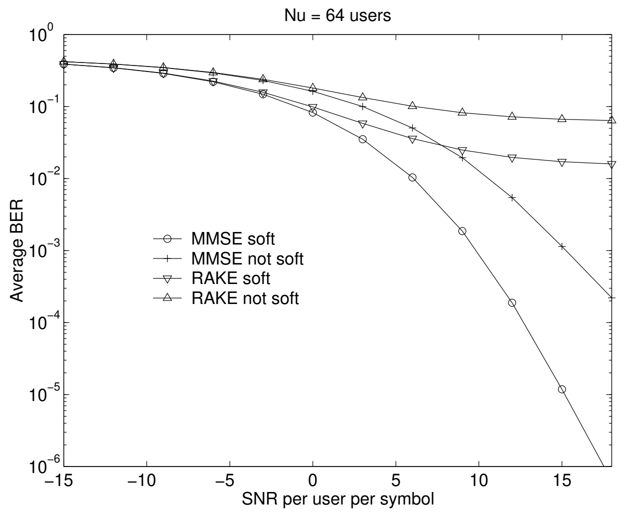

Figure 8: Uncoded BER results, 64 users, 2 base-stations

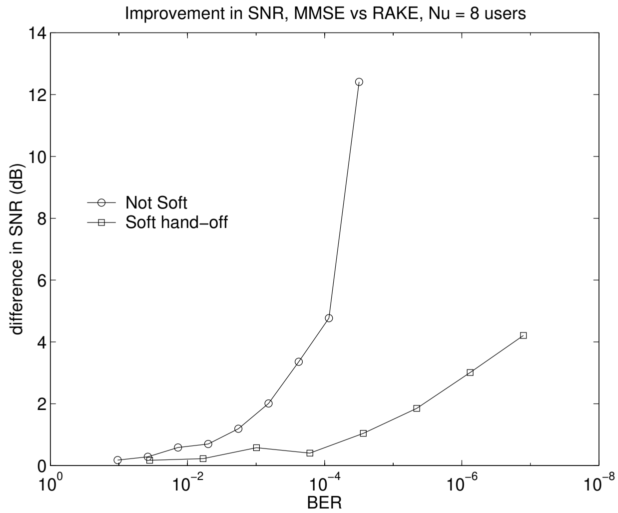

Figure 9: Improvement in SNR, 8 users

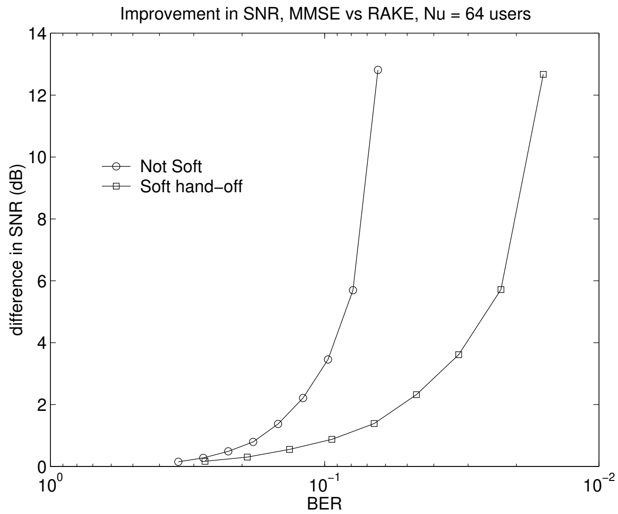

Figure 10: Improvement in SNR, 64 users

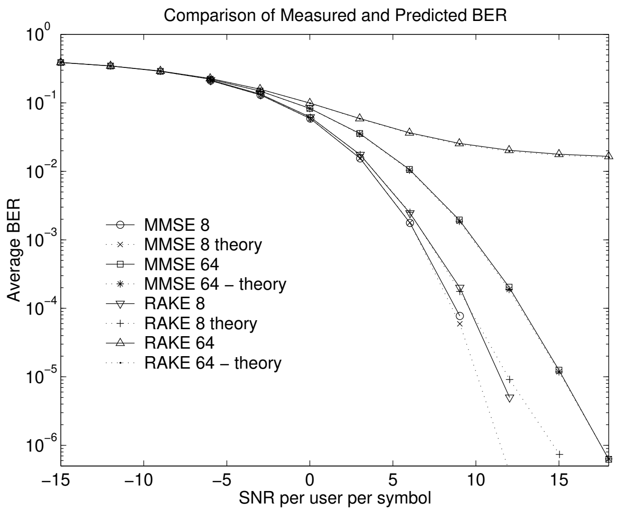

Figure 11: Validation of BER analysis, soft hand-off mode

the symbol-level and chip-level sets the symbol-level equalizer to $N_c + N_g - 1$ chips. Note that while this is a fair comparison if equalizer length mainly determines the computation (as might be the case for adaptive equalization), a "block" implementation involving actual matrix inversion in Equations 21 and 46 would require a larger matrix inverse for the symbol-level than for the chip-level. Figure 12 presents the results for the fully loaded cell case, i.e. 64 equal power users were simulated. The RAKE receiver is significantly degraded at high SNR by the MAI, which is seen in the Figure as a BER floor for SNR greater than 10 dB. The chip- and symbol-level equalizers perform much better than the RAKE. Increasing the equalizer length improves performance for both chip-level and symbol-level. Comparing the length 57 chip-level to 120 symbol-level, we observe little improvement in the symbol level at low SNR with increasing improvement, up to 2-3 dB, at high SNR. Comparing length 114 chip-level to 177 symbol-level also shows an improvement that increases with SNR, but less of an improvement than for the shorter equalizers. Note that since all 64 channel codes are present and have equal power, $\mathbf{R}_{SS} = \mathbf{I}$ and the symbol-level MMSE estimate is optimal in the MSE sense.

In Figure 13, once again the out-of-cell interference is assumed negligible. In this simulation only 8 equal power channel codes are active, i.e., the cell is only lightly to moderately loaded. In this simulation the RAKE receiver does much better since it experiences less in-cell MAI than for 64 users. For the range of SNR simulated the chip-level equalizer does only slightly better than the RAKE receiver. As for the fully loaded cell, the symbol-level equalizer performs better than the chip-level equalizer. For comparison the "optimal" symbol-level equalizer is shown which involves a matrix inverse for every symbol (as in Equation (46)); this equalizer is only slightly better than the symbol-level equalizer presented in this paper. This result justifies the assumption / simplification that $\mathbf{R}_{SS}$ is proportional to $\mathbf{I}$, even when $N_u < N_c$. This is despite the much greater computational complexity required for the optimal symbol-level equalizer: it must compute and invert the covariance $\mathbf{R_{SS}}[\mathbf{n}]$ for $n = mN_c + D$ for *all* $m = 0, 1, 2, \ldots$ (that is, for every symbol), whereas the non-optimal symbol-level equalizer need not do so.

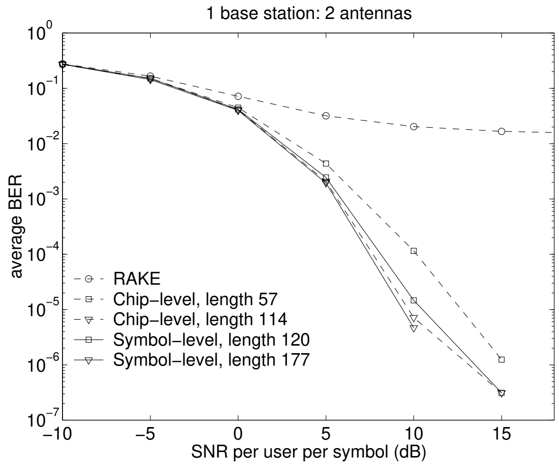

Figure 12: Fully loaded cell, all 64 channel codes in use.

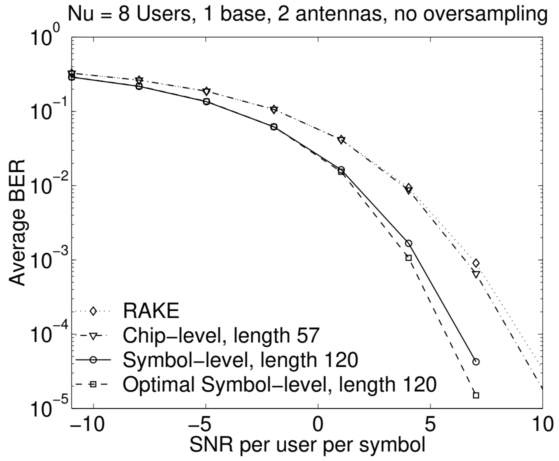

Figure 13: Lightly loaded cell, 8 out of 64 active channel codes.

7.4 Coded BPSK

In Figure 14 the soft hand-off receiver BER is compared for coded and uncoded signaling. For the coded system, a standard rate 1/2 convolutional code with constraint length 7 was employed. The generator polynomials were (171, 133) in octal. A Viterbi algorithm with survivor length 100 was used to decode the perturbed code symbols ("soft decisions") from the length $N_g = 57$ chip equalizer followed by decorrelator. The coded SNR has been increased by 3 dB to account for the increased signal energy per data bit. 500 channels were generated and 50 information bits (100 BPSK code bits) per channel per user were simulated; the actual BER was measured for all 64 users. As expected both RAKE and MMSE benefit from the error control coding at high SNR. From the Figure we see that the RAKE receiver in the coded case still exhibits an error floor, although at a much lower BER of about 10^{-5}. The MMSE equalizer achieves a much lower BER, consistent with the uncoded results. **In the case of data transmission where the target BER after coding is 10^{-6}, the advantage of MMSE equalization over the RAKE receiver is dramatic; in fact, RAKE cannot achieve this BER.**

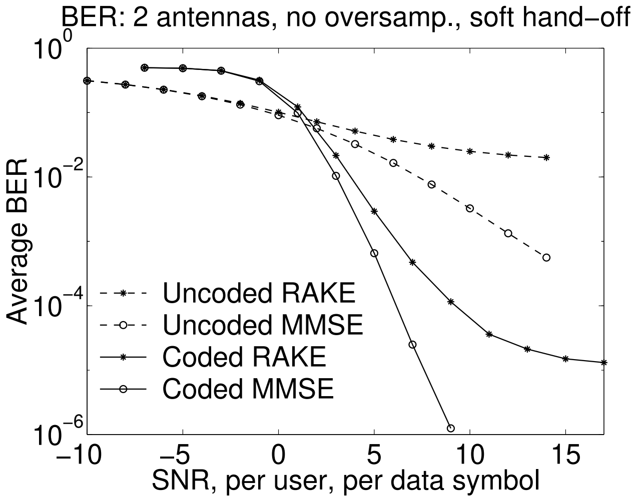

Figure 14: Comparison of average BER for coded and uncoded systems.

7.5 Uncoded 16-QAM

Future CDMA systems may employ higher order constellations, for example, Qualcomm's HDR system [22]. See also [23] for a comparison of 16-QAM and QPSK multiuser receivers in severe multipath. In such systems the MMSE downlink equalizer can significantly enhance performance over the RAKE receiver. Figures 15 and 16 present uncoded 16-QAM BER results. 500 channels were generated and 100 symbols (400 bits) per channel per user simulated; the actual BER results were averaged for all 64 users. There were two antennas, each with two times oversampling. The equalizer length was $N_g = 100$. The SNR has been reduced by a factor of 4 (6 dB) to account for the smaller signal energy per bit. Figure 15 shows the results for a single base-station in which out-of-cell interference is negligible. The MMSE equalizer significantly out-performs the RAKE. In this case the RAKE BER floor at high SNR is above .1 because 16-QAM suffers from residual interference. Figure 16 shows the results for two base-stations in soft hand-off operation. Again, the MMSE out-peforms RAKE but to a lesser degree since the second base-station in each of the two sections of the soft hand-off receiver contributes some interference.

7.6 Orthogonal Variable Spreading Factor (OVSF) Codes

The simulation results plotted in Figure 17 reveal the substantial performance gains of a chip-level MMSE Equalizer over a RAKE receiver in the case where OVSF codes are employed. In this simulation, there were thirty-two active channel codes with 64 chips per bit plus a single 2 chips per bit channel code. Each of the thirty-two codes of length 64 employed is orthogonal to each and every integer multiple of 2 time-shift of

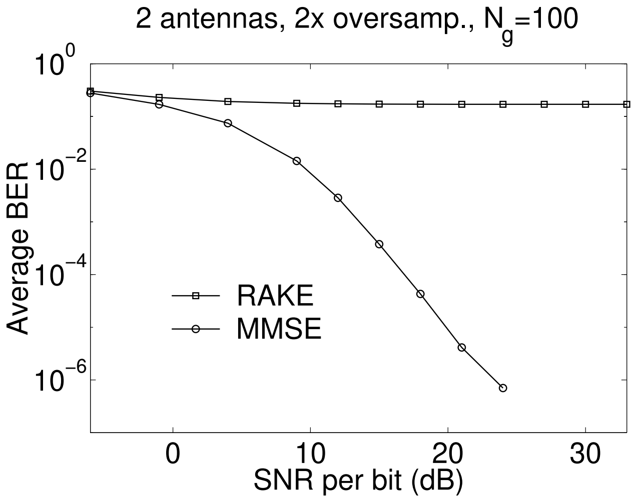

Figure 15: Comparison of average uncoded BER for RAKE and MMSE, 16-QAM constellation: ONE BASE-STATION

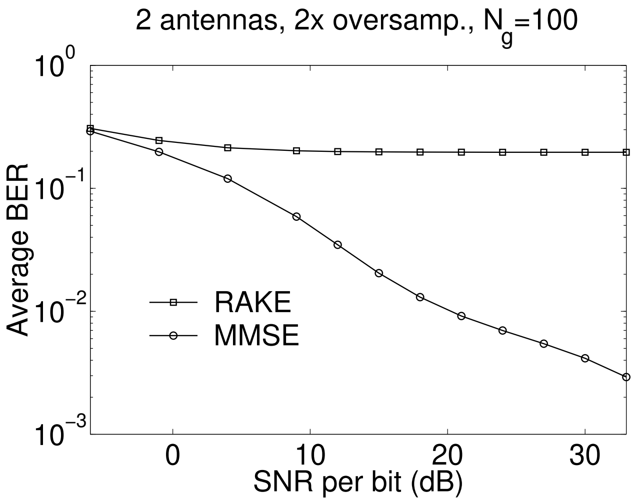

Figure 16: Comparison of average uncoded BER for RAKE and MMSE, 16-QAM constellation: TWO BASE-STATIONS (soft hand-off mode).

the single code of length 2. Two antennas were employed with no oversampling; out-of-cell interference was not simulated (only one base-station). The definition of SNR is slightly different for this scenario. SNR is here defined to be the signal to noise ratio for a given user PRIOR to the channel. This means that the channel and equalizer gain modify the power of the signal, while the noise power is modified only by the equalizer. For this simulation the channel consisted of 4 equal power paths, each arriving exactly at a chip interval. Each path had independent real and imaginary parts with unit variance, meaning each path has a power of 2. Because each of the four paths has the same strength at each of the two antennas, and all paths have at least a chip spacing between them, the RAKE receiver benefits from roughly a $10\log(8 \cdot 2) = 12$ dB diversity gain. Note that in practice the achievable diversity gain depends heavily on the actual multipath parameters and accurate estimation of them.

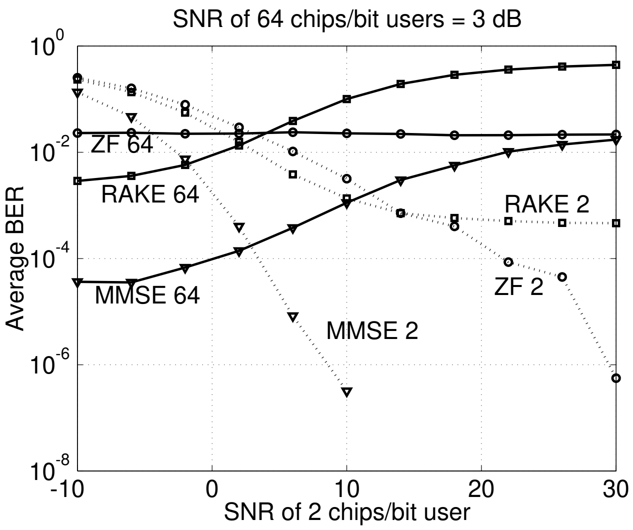

Figure 17: OVSF Simulation Results

The post-correlation SNR (defined as the SNR times the processing gain) for EACH of the thirty-two 64 chips per bit users (including $N_c = 64$ times (18 dB) processing gain) was held constant at 3 dB. The BER performance of the RAKE receiver, chip-level MMSE equalizer, and the ZF equalizer for the single 2 chips per bit user as a function of the post-correlation SNR of the single 2 chips per bit user (including 3 dB processing gain) is plotted in Figure 17 - see the curves labeled “RAKE 2”, “MMSE 2”, and “ZF 2”, respectively. In the 3 to 10 dB SNR range, the MMSE equalizer is observed to provide several orders of magnitude improvement in uncoded BER for the single 2 chips per bit user. Note that the performance of the RAKE receiver for the 2 chips per bit user suffers from inter-symbol interference as well as multipath-induced MAI since the delay spread is 37 chips corresponding to a delay spread of roughly a half-symbol.

In addition, Figure 17 plots the average BER performance of the RAKE receiver, the MMSE equalizer, and the ZF Equalizer for EACH of the thirty-two 64 chips per bit users as a function of the post-correlation

SNR of the single 2 chips per bit user - see the curves labeled “RAKE 64”, “MMSE 64”, and “ZF 64”, respectively. The BER performance of the ZF equalizer for each of the thirty-two 64 chips per bit users is observed to remain relatively constant as the SNR of the single 2 chips/bit user is increased due to the restoration of channel code orthogonality. In contrast, the BER performance of the RAKE receiver for each of the thirty-two 64 chips per bit users is observed to increase dramatically as the SNR of single 2 chips per bit user is increased, since this increases the level of the MAI affecting each of the thirty-two 64 chips per bit users.

As the SNR of the single 2 chips per bit user is increased, the point at which the BER of the single 2 chips per bit user is the same as that for EACH of the thirty-two 64 chips per bit users occurs at roughly the same SNR for all three different methods. Interestingly, this cross-over point occurs when the post-correlation SNR (includes 3 dB processing gain) of the single 2 chips per bit user is equal to the post-correlation SNR (includes 18 dB processing gain) of EACH of the thirty-two 64 chips per bit users: 3 dB. However, the BER at this cross-over point achieved with the chip-level MMSE equalizer is two orders of magnitude lower than the cross-over point BER achieved with either the RAKE receiver or ZF equalizer. These simulation results are a strong testament to the efficacy of employing an MMSE based chip-level equalization in the case of synchronous CDMA with OVSF channel codes.

7.7 One Versus Two Antennas

In this section we compare performance for one and two antenna systems. Two times oversampling was employed, yielding a total of two chip-spaced “virtual channels” in the one antenna case, and four in the two antenna case. SNR is once again according to the original definition. The results of the simulations for soft hand-off mode are plotted in Figure 18, and without soft hand-off (normal operation) in Figure 19. For the MMSE equalizers, two lengths were tried, length 57 (equal to the total channel length including tails) and twice that. The main result is that for this edge-of-cell, soft-hand-off situation, two antennas at the mobile-station can dramatically improve the average BER performance over a single antenna. Increasing the equalizer length helps, but does not bring the performance of the single antenna receiver anywhere near two antennas. Also, the relationship between RAKE and MMSE, and different equalizer lengths, holds whether in soft hand-off mode or in normal mode; soft hand-off simply improves the situation significantly as can be expected.

The dramatic enhancement in performance in the two antenna case can in part be explained through a linear-algebraic / zero-forcing argument. The channel matrix $\boldsymbol{\mathcal{H}}$ has dimension $MN_g \times 2(L + N_g - 1)$. With $M = 4$ channels and a per channel equalizer length equal to the channel length, $N_g = L$, $\boldsymbol{\mathcal{H}}$ is $4L \times 4L - 2$ (tall). This allows a left-inverse, or zero-forcing (ZF) solution, implying perfect cancellation of ISI (inter-“chip symbol” interference) *and* CCI (co-channel interference from the other base-station) in the case of no noise. Of course, in the practical case of noise, we employ the MMSE estimator over the ZF

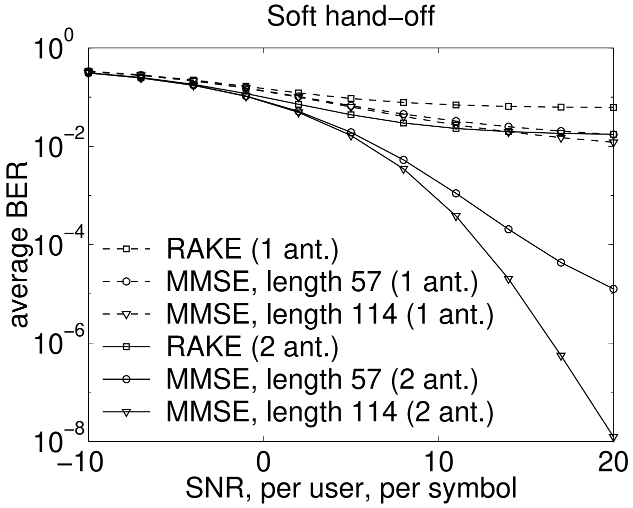

Figure 18: Soft-hand-off receiver, average BER performance.

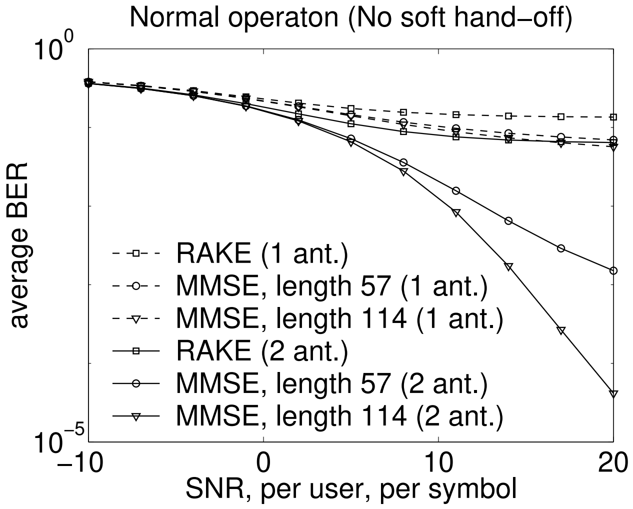

Figure 19: Normal mode (no soft-hand-off) receiver, average BER performance.

equalizer to avert high noise gains arising in the case where the respective 4 channels for either base-station have common or near common zeroes. That is, ZF considerations guide the choice of both the number of channels and the equalizer length per channel, but the MMSE estimator is used for equalization to avert potential high noise gains. Note that when the noise power approaches 0, the MMSE equalizer approaches the ZF equalizer (see Section 3.3) if there are no common zeroes amongst the channels.

Continuing the discussion of the two antenna case, it can be shown that the two polyphase channels created from either antenna are nearly linearly dependent in the case of a sparse multipath channel as encountered in the high-speed link simulated here. Thus, even though $\boldsymbol{\mathcal{H}}$ is tall with $M = 4$ channels and a per channel equalizer length equal to the channel length, thereby allowing a left-inverse and perfect zero-forcing (ZF), in the case of sparse multipath channels the resulting $\boldsymbol{\mathcal{H}}$ is ill-conditioned. ISI and CCI cancellation can be enhanced by increasing the per channel equalizer length above the channel length thereby facilitating inversion of the two nearly common polyphase channels extracted from either antenna. The simulation results reveal that doubling the per channel equalizer length from $L = 57$ to $N_g = 114$ yields a substantial performance enhancement.

In contrast, in the single antenna case ($M = 2$), both for $N_g = L$ and $N_g = 2L$, $\boldsymbol{\mathcal{H}}$ is wide ($2L \times 4L - 2$ and $4L \times 6L - 2$ respectively), and no zero-forcing solution exists. Further increases in the per channel equalizer length above $N_g = 2L$ yields diminishing returns as the use of two polyphase channels extracted from a single antenna does not provide enough degrees of freedom to cancel the multi-user access interference from the other base-station as well as cancel ISI.

If one extracts four polyphase channels from a single antenna, one can theoretically cancel co-channel interference as well as ISI. However, again, in the case of sparse multipath channels, the four polyphase channels from a single antenna are too linearly dependent to achieve this practically, especially in the practical case where the excess bandwidth associated with the chip pulse shaping is less than 50%. This is supported through simulating 500 channels and measuring the average BER for the soft hand-off receiver as seen in Figure 20. Four times oversampling with a single antenna does not improve the situation for either the RAKE receiver or the MMSE length 57 equalizer compared to just two times oversampling.

8 Conclusion

The results indicate that the MMSE chip-equalizers as recently developed have a great potential for increasing CDMA downlink capacity, and this result holds for the case of soft hand-off as well as normal operation. MMSE equalizers benefit greatly from multiple receive antennas. The SINR and BER analysis show that it is possible to theoretically predict the uncoded BER performance of 3G cellular systems under certain conditions, given knowledge of the channel or class of channels. The symbol-level equalizer derived here performs better than the chip-level, however at a greater computational cost. In fact our simulations have shown that even though the equalizer is sub-optimal, it has performance closely approaching the optimal

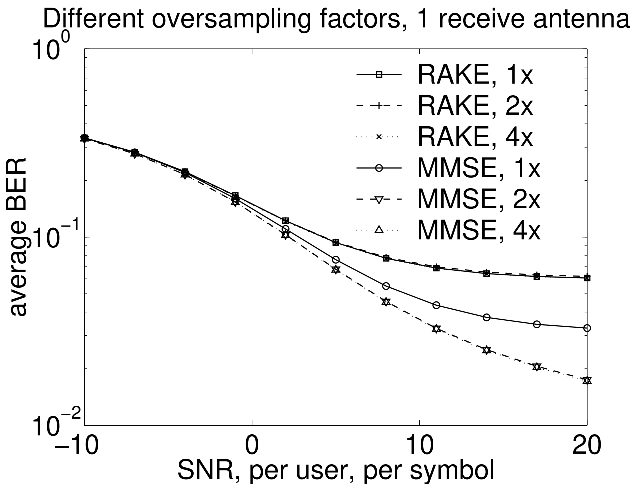

Figure 20: Comparison of 2x and 4x oversampling, 1 antenna.

linear equalizer. The approximation that the source covariance is diagonal means that a matrix inverse is required only as often as the channel changes (and not every symbol), and hence the computational complexity is much smaller than the optimal equalizer.

9 Acknowledgements

The authors thank Colin Frank and Eugene Visotsky at Motorola Labs for invaluable direction and sharing of ideas. Thanks to Geert Leus at the the Katholieke Universiteit Leuven, Belgium for early pointers into the benefits of MMSE equalization versus ZF and RAKE, even in the case of multiple channels. Also, thanks to Professor Saul Gelfand for use of his Sun HPC-450 and 3500 computers, which were obtained from the Army Research Office under the DURIP program. Thanks to Jeongsoon Park for discussions and resources on multiuser detection.

References

[1] Sergio Verdu, *Multiuser Detection*, Cambridge University Press, 1998.

[2] Anja Klein, "Data Detection Algorithms Specially Designed for the Downlink of CDMA Mobile Radio Systems", *in IEEE 47th Vehicular Technology Conference Proceedings*, pp. 203–207, Pheonix, AZ, 4-7 May 1997.

[3] Colin D. Frank and Eugene Visotsky, "Adaptive Interference Suppression for Direct-Sequence CDMA Systems with Long Spreading Codes", *in Proceedings 36th Allerton Conf. on Communication, Control, and Computing*, pp. 411–420, Monticello, IL, 23-25 Sept. 1998.

[4] I. Ghauri and DTM. Slock, "Linear receivers for the DS-CDMA downlink exploiting orthogonality of spreading sequences", *in Conf. Rec. 32rd Asilomar Conf. on Signals, Systems, and Computers, Pacific Grove, CA,*, Nov. 1998.

[5] Kari Hooli, Matti Latva-aho, and Markku Juntti, "Multiple Access Interference Suppression with Linear Chip Equalizers in WCDMA Downlink Receivers", *in Proc. Global Telecommunications Conf.*, pp. 467–471, Rio de Janero, Brazil, 5-9 Dec. 1999.

[6] Stefan Werner and Jorma Lilleberg, "Downlink Channel Decorrelation in CDMA Systems with Long Codes", *in IEEE 49th Vehicular Technology Conference Proceedings*, vol. 2, pp. 1614–1617, Houston, TX, 16-19 May 1999.

[7] M. Zoltowski and T. Krauss, "Two-Channel Zero Forcing Equalization on CDMA Forward Link: Trade-offs between Multi-user Access Interference and Diversity Gains", *in Conf. Rec. 33rd Asilomar Conf. on Signals, Systems, and Computers, Pacific Grove, CA*, 25-27 Oct. 1999.

[8] T. Krauss and M. Zoltowski, "Blind Channel Identification on CDMA Forward Link Based on Dual Antenna Receiver at Hand-set and Cross-relation", *in Conf. Rec. 33rd Asilomar Conf. on Signals, Systems, and Computers, Pacific Grove, CA,*, 25-27 Oct. 1999.

[9] T. Krauss, M. Zoltowski, and G. Leus, "Simple MMSE Equalizers for CDMA Downlink to Restore Chip Sequence: Comparison to Zero-Forcing and RAKE", *in International Conference on Acoustics, Speech, and Signal Processing*, 5-9 June 2000.

[10] Thomas P. Krauss and Michael D. Zoltowski, "MMSE Equalization Under Conditions of Soft Hand-Off", *in IEEE Sixth International Symposium on Spread Spectrum Techniques & Applications (ISSSTA 2000)*, NJIT, New Jersey, 6-8 September 2000.

[11] Thomas P. Krauss, William J. Hillery, and Michael D. Zoltowski, "MMSE Equalization for Forward Link in 3G CDMA: Symbol-Level Versus Chip-Level", *in Proceedings of the* 10^{th} *IEEE Workshop on Statistical Signal and Array Processing (SSAP 2000)* , Pocono Manor, PA, 14-16 August 2000.

[12] Thomas P. Krauss and Michael D. Zoltowski, "Chip-level MMSE Equalization at the Edge of the Cell", *in Proceedings of the IEEE Wireless Communications and Networking Conference (WCNC 2000)*, Chicago, IL, 23-28 September 2000.

[13] T. Krauss and M. Zoltowski, "Oversampling Diversity Versus Dual Antenna Diversity for Chip-Level Equalization on CDMA Downlink", *in Proceedings of First IEEE Sensor Array and Multichannel Signal Processing Workshop, Cambridge, MA*, 16-17 March 2000.

[14] G. Xu, H. Liu, L. Tong, and T. Kailath, "A least-squares approach to blind channel identification", *IEEE Trans. on Signal Processing*, vol. 43, pp. 2982–2993, Dec. 1995.

[15] Anthony J. Weiss and Benjamin Friedlander, "Channel Estimation for DS-CDMA Downlink with Aperiodic Spreading Codes", *IEEE Transactions on Communications*, vol. 47, pp. 1561–1569, Oct. 1999.

[16] A. Klein, G. Kaleh, and P. Baier, "Zero Forcing and Minimum Mean-Square-Error Equalization for Multiuser Detection in Code-Division Multiple-Access Channels", *IEEE Transactions on Vehicular Technology*, vol. 45, pp. 276–287, May 1996.

[17] Wireless Valley Communications, Inc., *SMRCIM Plus 4.0 (Simulation of Mobile Radio Channel Impulse Response Models) User's Manual*, 24 Aug. 1999.

[18] D. H. Brandwood, "A complex gradient operator and its application in adaptive array theory", *IEE Proc., Parts F and H*, vol. 130, pp. 11–16, Feb. 1983.

[19] Thomas Kailath, *Linear Systems*, Prentice Hall, 1980.

[20] Hui Liu and Mike Zoltowski, "Blind equalization in antenna array CDMA systems", *IEEE Transactions on Signal Processing*, vol. 45, pp. 161–172, Jan. 1997.

[21] Telecommunications Industry Association TIA, "Physical Layer Standard for cdma2000 Standards for Spread Spectrum Systems - TIA/EIA/IS-2000.2-A", TIA/EIA Interim Standard, March 2000.

[22] A. Julali, R. Padovani, and R. Pankaj, "Data Throughput of CDMA-HDR a High Efficiency-High Data Rate Personal Communication Wireless System ", *in Proc. of IEEE Vehicular Technology Conference*, Tokyo, Japan, 15–18 May 2000.

[23] Prasad Shamain and Laurence B. Milstein, "Using higher order constellations with minimum mean square error (MMSE) receiver for severe multipath CDMA channel", *in Proceedings of Ninth IEEE International Symposium on Personal, Indoor and Mobile Radio Communications*, pp. 1035–1039, Boston, MA, 8-11 Sept. 1998.